J. Am. Soc. Mass Spectrom. (2015) 26:2152–2161
DOI: 10.1007/s13361-015-1245-4

RESEARCH ARTICLE

Analysis of Native-Like Proteins and Protein Complexes Using Cation to Anion Proton Transfer Reactions (CAPTR)

Kenneth J. Laszlo, Matthew F. Bush

Department of Chemistry, University of Washington, Seattle, WA 98195-1700, USA

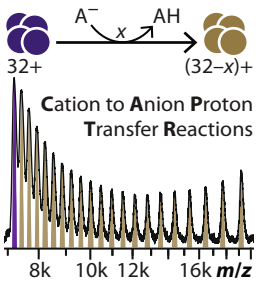

Abstract. Mass spectra of native-like protein complexes often exhibit narrow charge-state distributions, broad peaks, and contributions from multiple, coexisting species. These factors can make it challenging to interpret those spectra, particularly for mixtures with significant heterogeneity. Here we demonstrate the use of ion/ion proton transfer reactions to reduce the charge states of *m/z*-selected, native-like ions of proteins and protein complexes, a technique that we refer to as cation to anion proton transfer reactions (CAPTR). We then demonstrate that CAPTR can increase the accuracy of charge state assignments and the resolution of interfering species in native mass spectrometry. The CAPTR product ion spectra for pyruvate kinase exhibit ~30 peaks and enable unambiguous determination of the charge state of each peak, whereas the corresponding precursor spectra exhibit ~6 peaks and the assigned charge states have an uncertainty of ±3%. 15+ bovine serum albumin and 21+ yeast enolase dimer both appear near *m/z* 4450 and are completely unresolved in a mixture. After a single CAPTR event, the resulting product ions are baseline resolved. The separation of the product ions increases dramatically after each subsequent CAPTR event; 12 events resulted in a 3000-fold improvement in separation relative to the precursor ions. Finally, we introduce a framework for interpreting and predicting the figures of merit for CAPTR experiments. More generally, these results suggest that CAPTR strongly complements other mass spectrometry tools for analyzing proteins and protein complexes, particularly those in mixtures.

Keywords: Native mass spectrometry, Ion/ion chemistry, Ion chemistry, Proton transfer reactions, Protein complexes

Received: 12 June 2015/Revised: 23 July 2015/Accepted: 1 August 2015/Published Online: 1 September 2015

Introduction

Most electrospray ionization mass spectrometry experiments of proteins use denaturing solutions containing acidified mixtures of aqueous and organic solvents, which disrupt the structures of proteins and yield a wide distribution of highly charged molecular ions. Alternatively, proteins can be electrosprayed from a "native" aqueous solution that contains a volatile electrolyte (e.g., ammonium acetate or ammonium bicarbonate) and has a physiologically relevant pH and ionic strength. The ions formed in such native mass spectrometry experiments have been shown to retain the stoichiometry of proteins, ligands, and metal ions of the corresponding noncovalent complexes in solution [1–4], and are often referred to as native-like ions. Results from native mass spectrometry experiments are now used in a wide range of structural biology applications, including investigations of the formation of amyloids [5, 6], bacterial secretion [7, 8], protein oligomerization [9], small heat shock protein structure [10, 11], and viral capsid assembly [12–14].

Native mass spectra of proteins and protein complexes exhibit relatively narrow charge state distributions that appear at high *m/z* values compared to those for ions generated from denaturing solutions, which make charge-state assignments more challenging [12]. This is exacerbated for heterogeneous samples, which yield congested mass spectra [10]. Several computational approaches have been implemented to aid in the interpretation of protein mass spectra [11, 15–20], including methods that use functions to simulate a spectrum and whose parameters are optimized to minimize the deviation with the experimental spectrum [11, 17, 19, 20] and those that translate the *m/z* axis to an *m* axis [15, 16, 18]. Tandem mass spectrometry is used extensively to elucidate the identities of

Electronic supplementary material The online version of this article (doi:10.1007/s13361-015-1245-4) contains supplementary material, which is available to authorized users.

Correspondence to: Matthew Bush; *e-mail:* mattbush@uw.edu

precursor ions in native mass spectrometry, although the pathways and efficiencies of dissociation can depend strongly on the timescale of energy deposition [21], charge state [22], and subtle aspects of the dissociation process [23]. Furthermore, there are numerous examples of noncovalent protein complexes that could not be dissociated via subunit loss using collision-induced dissociation [22, 24–26].

Another experimental approach for interpreting electrospray ionization mass spectra is to form additional charge states of the analyte, thus enabling complementary measurements of *m/z*. For example, additional charge states can be observed when supercharging or charge-reducing agents are added to electrospray solutions [27–31]. Alternatively, gas-phase proton transfer reactions offer a facile means to modulate the charge states of multiply charged ions. One option is to react a multiply charged precursor cation with a neutral molecule, A, which has a higher gas-phase basicity (ion/neutral proton transfer reactions) [32, 33]:

$$[M_n + xH]^{x+} + A \rightarrow [M_n + (x-1)H]^{(x-1)+} + AH^+ \quad (1)$$

The rates of these reactions are limited by the weak interaction of the reactants at long distances and the relative basicities of the reactants. Furthermore, molecules that have high gas-phase basicities typically also have low volatilities, which (1) limits the range of pressures that can be used, and (2) causes those molecules to persist after experiments due to adsorption on the walls of vacuum systems.

A second option is to react a multiply charged precursor cation with an anion (ion/ion proton transfer reactions) [34–39]:

$$[M_n + xH]^{x+} + A^- \rightarrow [M_n + (x-1)H]^{(x-1)+} + AH \quad (2)$$

The rates of these reactions benefit from long-range Coulombic interactions between the reactants and that the reaction remains exothermic even after a series of reactions [40, 41]. Positioning an α emitter [37] or a corona discharge [38, 39] immediately after the analyte ionization source can enable extensive charge reduction of all analyte ions. Performing ion/ion proton transfer reactions inside mass spectrometers offers additional advantages because ions can be manipulated prior to charge reduction [42] (e.g., ion activation, chemistry, or *m/z* selection). In the context of native mass spectrometry, performing ion/ion proton transfer reactions in vacuum decouples the ionization and charge manipulation processes so as to not compromise solution chemistry, noncovalent interactions, or the ionization process. Pathways other than proton transfer may also be accessible in ion/ion reactions [36, 43] (e.g., electron transfer and anion adduction).

Here, we demonstrate the use of ion/ion proton transfer reactions of quadrupole selected, native-like ions, which we refer to as cation to anion proton transfer reactions (CAPTR). We then use CAPTR to (1) assign accurately the charge states of native-like precursor ions, and (2) separate two native-like precursor ions that are not initially resolved in *m/z*. These results indicate that CAPTR will increase the accuracy of a broad range of native mass spectrometry experiments.

Experimental

Experiments were performed using a Waters Synapt G2 HDMS mass spectrometer (Wilmslow, United Kingdom) modified with a glow-discharge ionization source [44] (Figure 1a). Native-like cations were generated using nanoelectrospray ionization from borosilicate capillaries with inner diameters of 0.78 mm that were pulled to ~1–3 μm on one end using a Sutter Instruments Model P-97 micropipette puller (Novato, CA, USA). Electrical contact with the solution was achieved by inserting a platinum

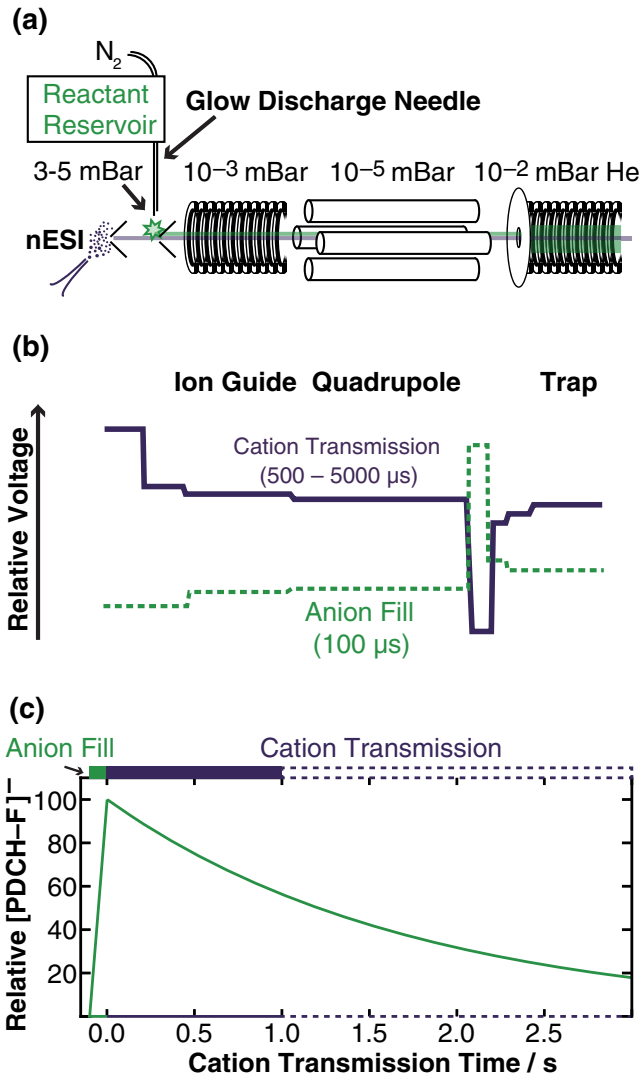

Figure 1. **(a)** Waters Synapt G2 HDMS modified with glow-discharge ionization source. **(b)** Relative potentials applied to selected ion optics during cation transmission (*solid purple line*) and anion fill (*dashed green line*). **(c)** Hypothetical abundance of $[PDCH - F]^-$ in the trap cell over the course of a single experimental cycle

wire into the wide end of the capillary. Electrospray solutions contained ~10 μM protein or protein complex in 200 mM aqueous ammonium acetate pH = 7. Yeast enolase, alcohol dehydrogenase, and pyruvate kinase were also buffer exchanged into the same buffer using Micro Bio-Spin 6 columns (Bio-Rad, Hercules, CA, USA). Insulin was electrosprayed from 49.5/49.5/1 methanol/water/acetic acid. The atmospheric pressure interface was held at 120°C.

For CAPTR experiments, nitrogen gas seeded with perfluoro-1,3-dimethylcyclohexane (PDCH) vapor was passed through a sharpened stainless steel discharge needle that was positioned after the atmospheric pressure sampling cone (pressure ~4 mbar). Anions were generated for 100 ms, which will be referred to as the anion fill time, by applying a 0.2–1.3 kV potential to the discharge needle that induces a discharge current of 10–100 μA. $[PDCH–F]^-$ was selected using a quadrupole mass filter and accumulated in a stacked ring ion trap cell, which contained ~0.01 mbar of He gas. Cations were then transmitted for ~2000 ms, which will be referred to as the cation transmission time, through the trap cell containing the accumulated anions. The charge-reduced products and any residual precursor cations continue through the radio-frequency confining drift cell [31], stacked-ring collision cell, and time-of-flight mass analyzer. To increase the detection efficiency of high *m/z* ions, the magnitude of the detector voltage was increased 300–475 V above that used for peptide analysis. The relative potentials of the ion optics that are modulated between the anion fill and cation transmission times are shown in Figure 1b. During the cation transmission time, the amplitude of the traveling waves in the trap cell was held at 0 V to maximize cation and anion spatial overlap. Representative time scales and hypothetical relative abundance of $[PDCH–F]^-$ over the course of the experiment are shown in Figure 1c.

Results and Discussion

Cation to Anion Proton Transfer Reactions (CAPTR)

CAPTR experiments were implemented using a dual polarity electrospray/glow-discharge ionization source that was positioned prior to a quadrupole mass filter, stacked-ring ion trap cell, radio-frequency confining drift cell [31], stacked-ring collision cell, and time-of-flight mass analyzer (Waters Synapt G2 HDMS) (Wilmslow, United Kingdom). Compared to previous instruments that have been used for ion/ion proton transfer reactions, this geometry is most similar to that reported by Badman and coworkers who used multiple independent ion sources positioned prior to a 3D ion trap, ion mobility drift tube, quadrupole collision cell, and time-of-flight mass analyzer [45]. The experimental scheme for CAPTR experiments, including the instrument, the relative potentials of selected ion optics, and the sequence are shown in Figure 1.

Figure 2a shows a typical native mass spectrum of avidin, a 64 kDa homotetramer, which exhibits peaks for the 15+ to 18+ charge states. CAPTR experiments were performed on the quadrupole selected 17+ charge state of avidin with an anion fill time of 100 ms and a cation transmission time of 500 ms. Note that the cation transmission time of 500 ms is the time that the cation beam is transmitted through the trap cell containing the anion; the interaction time between the cations and anions in these experiments is shorter and has not yet been

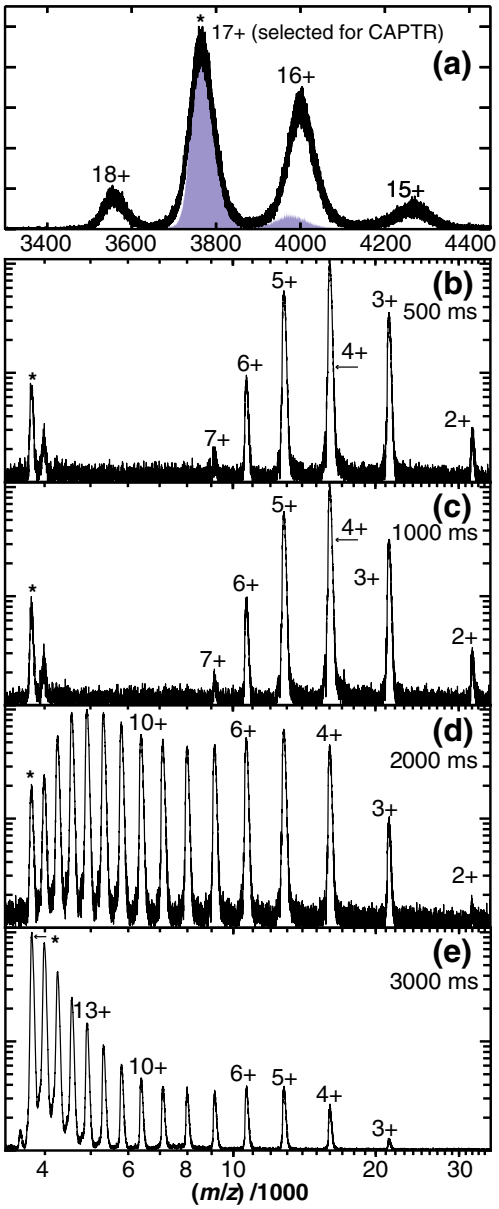

Figure 2. **(a)** Native mass spectrum of the avidin tetramer (64 kDa) plotted using linear axes. The spectrum obtained after precursor selection is shown in solid purple. CAPTR spectra of 17+ avidin measured using an anion fill time of 100 ms and cation fill times of **(b)** 500, **(c)** 1000, **(d)** 2000, and **(e)** 3000 ms. Spectra (**b**–**e**) are plotted using logarithmic axes to aid in visualization. The 17+ precursor ion is labeled with an "*". Average *z* for panels (**a**–**e**) are 16.3, 4.4, 4.5, 9.6, and 14.7 respectively. The relative intensities based on ion counting are shown in Electronic Supplementary Material Figure S1

characterized. The resulting CAPTR spectrum is shown in Figure 2b and exhibits peaks for 2+ through 7+ CAPTR product ions, which are the result of a series of consecutive proton transfer reactions (Reaction (2)) from the multiply charged protein cation to $[PDCH–F]^-$. The relative intensities based on ion counting are shown in Electronic Supplementary Material Figure S1F; almost 50% of the CAPTR products observed were for the 4+ product ion.

Of all of the avidin cations shown in Figure 2b, 97% are the result of 10–15 CAPTR events (2–7+, Electronic Supplementary Material Figure S1F). The intensity of any 8–15+ cations account for less than 1% of the total. Finally, 1.7% underwent no charge reduction (the residual 17+) and 0.5% lost one charge (16+). Figure 2a also shows the spectrum obtained without glow discharge ionization, with all other instrument parameters identical to those used to obtain Figure 2b. This spectrum also exhibits a minor peak for 16+ avidin; analogous features are commonly observed in native mass spectrometry experiments [46] and are attributed to pathways other than CAPTR. Interestingly, the peak observed for 16+ avidin without glow-discharge ionization appears at a slightly lower m/z than that formed directly from electrospray. The abundance of the 16+ relative to the 17+ in Figure 2b is roughly 3-fold higher than that observed without glow-discharge ionization, indicating that the 16+ ions formed in the CAPTR experiments includes subpopulations that underwent a single CAPTR event and that experienced background charge reduction. Since most precursor ions undergo extensive charge reduction in these experiments, these results suggest that a small fraction (~2%) of the precursor ions do not fully interact with the trapped anions. The origin of this effect is under investigation.

Kinetics and Pathways of CAPTR

To investigate how the experimental sequence affects CAPTR, the cation transmission time was modulated from 500 to 3000 ms (Figure 2b–e, normalized intensities are plotted in Electronic Supplementary Material Figure S1F–I). Note that although the cation transmission time is modulated, the residence time (and thus the reaction time) of a single ion in the trap cell is expected to be constant. The spectra recorded for CAPTR of 17+ avidin with cation transmission times of 500–1000 ms (Figure 2b and c) are indistinguishable. In contrast, the spectrum recorded with a cation transmission time of 2000 ms (Figure 2d) is significantly different and exhibits peaks for the 2+ through 16+ CAPTR products. This trend continues when the cation transmission time is further increased to 3000 ms (Figure 2e); the products observed under those conditions, on average, are the result of even fewer CAPTR events.

The similarity between the spectra measured using shorter (≤1000 ms) cation transmission times suggests that there is a large excess of anions and the abundance of anions in the trap cell does not change significantly during the first second of cation transmission (i.e., the reactions occur with pseudo-first-order kinetics). Pseudo-first-order kinetics have been reported for many ion/ion chemistry reactions performed in quadrupolar ion traps [47] and transmission mode experiments performed using a modified triple quadrupole [48] during the analysis of comparatively small biomolecules. Under pseudo-first-order kinetics, rates for these reactions have been shown to increase with the square of the charge state (z^2) [47].

The appearance of additional product ions that have undergone fewer CAPTR events with longer cation transmission times suggests that the abundance of $[PDCH–F]^-$ in the trap cell decreases significantly over the course of the longer experimental cycles (Figure 2c and d). Anions are refilled more frequently in most ion trap experiments in order to maintain pseudo-first-order reaction conditions [36], although subtle deviations from the pseudo-first-order kinetic model have been attributed to the depletion of anions in some cases [49]. The range of kinetic rates in these CAPTR experiments therefore enables the formation of an extremely broad range of charge-reduced product ions in a single experiment.

To evaluate whether the number of CAPTR events may be limited by the thermodynamics of Reaction (2), the gas-phase basicities of $[PDCH–F]^-$ were calculated at the B3LYP/6-31++G(d,p) level of theory. Detailed methods and results for these calculations are included in the Electronic Supplementary Material. The smallest gas-phase basicity calculated using this approach was 1310 kJ/mol. By comparison, the gas-phase basicity of a lysine residue in a neutral peptide is far lower (1008–1018 kJ/mol) and will decrease with increasing charge state [33, 50]. The gas-phase basicity of isolated arginine is ~60 kJ/mol greater than that of isolated lysine [51]; therefore, 1080 kJ/mol should represent a reasonable upper limit to the gas-phase basicity of arginine in a peptide or protein. Thus, the transfer of a proton from the reactant protein cation to $[PDCH–F]^-$ should be >200 kJ/mol exothermic for each CAPTR event. The rates of these reactions are therefore limited by the cross section for the formation of a long-range interaction complex between the reactants [36, 43, 52] and the density of the anions, rather than their thermodynamics.

Despite the high exothermicity of these reactions, no significant fragmentation was observed from CAPTR, consistent with results for smaller analytes [49]. These results suggest that the energy released during each CAPTR event is dissipated through other pathways and/or the energy may not partition statistically into both products. Furthermore, it is clear that protein complexes maintain native-like oligomeric stoichiometries. Preliminary ion mobility results suggest that the collision cross sections of CAPTR product ions are generally similar to those of the native-like precursor ions. More detailed studies of the effects of CAPTR on protein ion structure are underway.

It is possible that reaction pathways other than proton transfer may be accessed in ion/ion reactions [36, 43], including electron transfer and anion adduction. Electron transfer dissociation (ETD) typically results in fragmentation along the peptide backbone between the nitrogen and α-carbon generating c^+ and $z^{+\bullet}$ ions, although cleavage of disulfide bonds has also been reported [53]. In some cases, dissociation may not follow bond cleavage due to noncovalent interactions tethering the fragment to the remainder of the ion (ETnoD). Following electron

transfer to native-like protein complex cations in previous studies, additional activation has been shown to release noncovalently bound c^+ and $z^{+\bullet}$ fragments [54–56]. The possible contributions from each of these pathways are assessed below.

To demonstrate that protein complex cations react with $[PDCH–F]^-$ via proton transfer rather than electron transfer, denatured insulin and native-like alcohol dehydrogenase ions were activated in the collision cell on the instrument following CAPTR (Electronic Supplementary Material Figures S2 and S3, respectively). Discussions of these results may be found in the Electronic Supplementary Material. Briefly, collision induced dissociation (CID) of the CAPTR products of insulin yielded the same product ions as CID of the precursor ions. No fragments in either experiment could be attributed to cleavage of a disulfide bond (Electronic Supplementary Material Figure S2). CID using up to a 150 V injection voltage of the precursor (Electronic Supplementary Material Figure S3D) and CAPTR products (Electronic Supplementary Material Figure S3E) of tetramers of alcohol dehydrogenase resulted in the ejection of a highly charged monomer. No evidence for the loss of peptide fragments from the tetramer was observed. In contrast, CID using a 15 V injection voltage of the ETnoD products of tetramers of alcohol dehydrogenase has been reported previously to result in the appearance of c^+ and $z^{+\bullet}$ fragments [56]. These results all indicate that reacting protein ions with $[PDCH–F]^-$ results in proton transfer, rather than electron transfer, consistent with previous results for smaller biomolecular ions [52].

Anion adduction was monitored through the mass distribution of the CAPTR products of avidin (Electronic Supplementary Material Figure S4). The weighted average mass of the CAPTR products of avidin increase slightly with decreasing charge. For example, the weighted average mass of 3+ avidin is 199 Da greater than that for the 17+ precursor ion, which is less than the mass of $[PDCH–F]^-$ (381 Da). This shift is significantly larger than the errors expected for calibration. These spectra were externally calibrated using $Cs(CsI)_n^+$ clusters that appeared from m/z 3,000 to 19,000, which resulted in residual errors spanning ±7 ppm. Although 3+ avidin (m/z 21,500) appears slightly above this range, this analysis suggests that the calibration error would be on the order of 0.5 Da. Therefore, the observed increase in average mass suggests that the 3+ product ions include unresolved populations that have adducted zero, one, or possibly two anions. Therefore, CAPTR is a much more dominant channel than anion adduction.

Assigning Charge States in Native Mass Spectrometry

Native mass spectrometry inherently involves high mass, multiply charged ions that have high m/z values. In native mass spectrometry, charge states are often assigned by analyzing the spacing between adjacent peaks that differ by one charge. However, as charge increases, the m/z difference between charge states decreases, which makes charge-state assignments ambiguous [12]. This problem is exacerbated by wide peaks and narrow charge-state distributions, which are common to native mass spectrometry experiments. For example, Figure 3a–c show a native mass spectrum of the pyruvate kinase homotetramer (black trace) that is assigned using spectra simulated for three models. Spectra that were simulated assuming that the charge state of the base peak is 31+, 32+, or 33+ (3a, 3b, and 3c, respectively) all agree reasonably well with the experimental spectrum. A description of these simulations is included with the ESM. Visually, the simulated spectrum for which the base peak was assigned as 31+ agrees best with the experimental spectrum. Note that uncertainty in the assignments of charge states corresponds to ambiguity in the mass of the protein complex, *e.g.* assigning the base peak 31+ results in a mass of 223.1 kDa, whereas assigning the base peak 32+ results in a mass of 230.1 kDa (Δm = 30,000 ppm or 3%).

To mitigate this limitation in native mass spectrometry, the additional peaks generated by CAPTR were used to aid in the assignment of the base peak in the original native mass spectrum of pyruvate kinase. The CAPTR spectrum exhibits peaks for both the precursor ion and a long distribution of charge-reduced product ions. Using the masses determined from the charge state assignments in Figure 3a–c, CAPTR spectra were simulated and plotted with the experimental CAPTR spectrum (Figure 3d–f). When the charge state of the precursor ion is assigned as the 31+ or 33+, the simulated CAPTR spectra disagree with the experimental CAPTR spectrum, even though spectra simulated using those assignments for the original native mass spectrum agree reasonably well. When the charge state of the precursor ion is assigned as 32+, the simulated CAPTR spectrum agrees well with the experimental CAPTR spectrum (Figure 3e). The additional charge states generated by CAPTR radically reduce the ambiguity of charge-state assignments. This reduces the uncertainty in the mass determination to the accuracy of the mass analyzer and the underlying heterogeneity in the mass of the protein ion (e.g., covalent modification of the proteins as well as nonspecific adduction of molecules and ions).

Resolution of Components in Congested Mass Spectra

In native mass spectrometry, it is common to observe the presence of multiple coexisting protein complexes that have different stoichiometries and masses. This causes spectral congestion, which makes it challenging to interpret the spectra, particularly for polydisperse species that adopt many coexisting stoichiometries [10]. Although experimental methods using collision-induced dissociation have been developed to deconvolute these congested spectra [10], this approach implicitly assumes that the product ion distributions have complete fidelity with the original distributions in solution. However, the efficiency of the low-energy thermal dissociation of protein complexes has been shown to depend on the analyte, often in ways that cannot be predicted a priori [22, 23]. In contrast, CAPTR reaction rates depend primarily on the

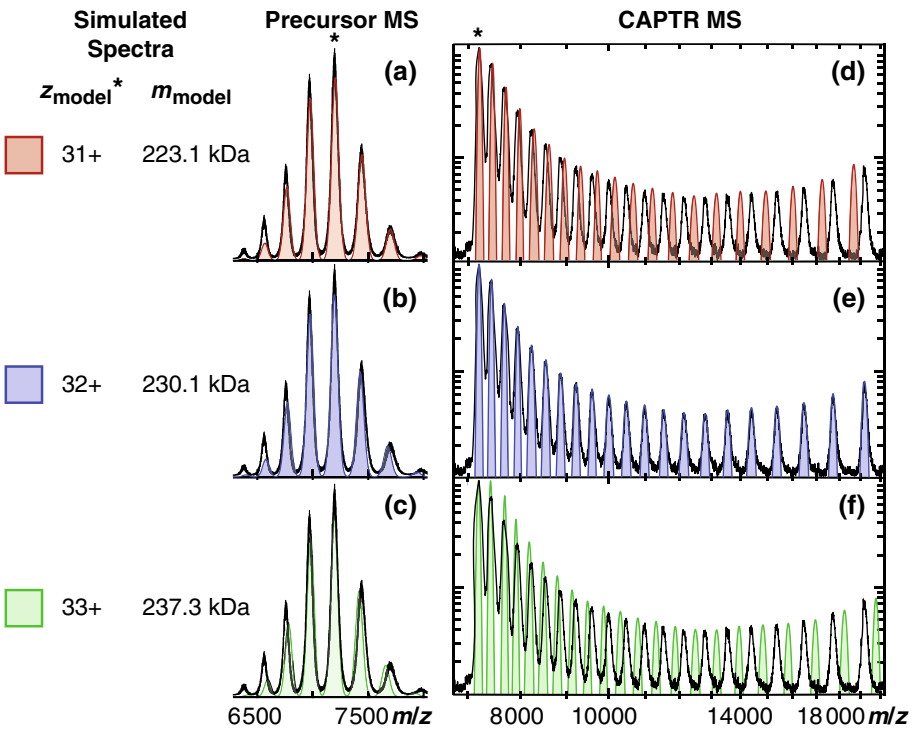

Figure 3. **(a)–(c)** each show a simulated spectrum that was used to model the experimental native mass spectrum of pyruvate kinase (*black*). Assigning the base peak at *m/z* 7200 a charge of 31+ (**a**, *red*), 32+ (**b**, *blue*), or 33+ (**c**, *green*) results in optimized masses of 223.1, 230.3, and 237.3 kDa, respectively; **(d)–(f)** each show a simulated spectrum that was used to model the experimental CAPTR spectrum for the *m/z* 7200 peak of pyruvate kinase. These spectra were simulated using the *m* determined for the corresponding model of the native mass spectrum. Intensities were set manually to resemble the intensities in the experimental spectrum

charge state of the analyte. This strategy is analogous to charge manipulation approaches pioneered by McLuckey and coworkers to analyze mixtures of comparatively small biomolecular ions in ion traps [32, 35, 47, 57].

To demonstrate the utility of CAPTR for separating interfering components in a mixture, bovine serum albumin (67 kDa monomer) and yeast enolase dimer (93 kDa) were analyzed. The resolution (R) between two peaks in a mass spectrum can be defined as:

$$Resolution = R = \frac{\frac{m_x}{z_x} - \frac{m_y}{z_y}}{2(\sigma_x + \sigma_y)} \quad (1)$$

where m, z, and σ are the mass, charge, and standard deviation for components x and y of the mixture. This definition of resolution is commonly used in chromatography to quantify the separation of two peaks in a chromatogram. Figure 4a shows overlaid native mass spectra of serum albumin (blue) and enolase dimer (green). The peaks for 15+ serum albumin and 21+ enolase dimer both appear near *m/z* 4450, and are completely unresolved (R = 0.016 << 1) in a mixture of serum albumin and enolase dimer. However, when the precursor ions near *m/z* 4450 are each isolated and subjected to CAPTR, the majority of the resulting product ions appear at unique *m/z* values (Figure 4b and c, respectively). These findings were then validated by performing CAPTR on the precursor ions near *m/z* 4450 that were isolated from a mixture of serum albumin and enolase (Figure 4d). Furthermore, these components are baseline resolved (R = 2.06) following a single CAPTR event (Figure 4e).

The resolution of CAPTR product ions were determined as a function of the number of CAPTR events from the results in Figure 4b and c. Briefly, the peaks in Figure 4b and c were each fit using a Gaussian distribution to determine the centroid and σ of each peak. These results show that the resolution increases dramatically with each subsequent CAPTR event (Figure 5a). After 12 CAPTR events, 3+ serum albumin and 9+ enolase dimer exhibit a resolution of 54, which is more than 3000-fold greater than that for the 15+ serum albumin and 21+ enolase dimer precursor ions. This analysis was also performed for the spectrum in Figure 4d. The resolution values determined in that analysis are similar to, but systematically smaller than, those determined in the previous analysis. This is attributed to the peaks in the spectrum obtained for the mixture having slightly greater widths than those measured in the spectra of

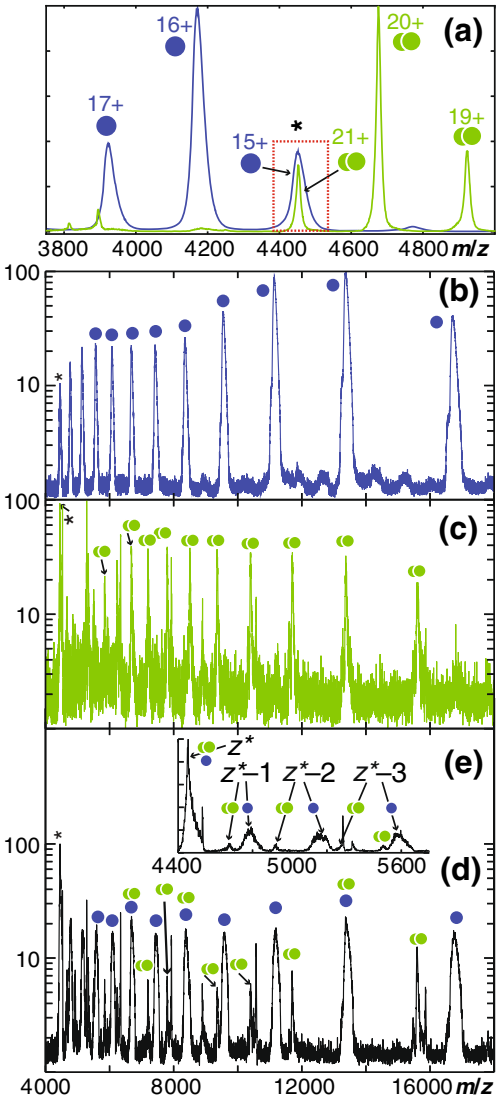

Figure 4. **(a)** Native mass spectra of bovine serum albumin (*blue*) and yeast enolase (*green*). **(b)** CAPTR of 15+ serum albumin. **(c)** CAPTR of 21+ enolase dimer. **(d)** CAPTR of 15+ serum albumin and 21+ enolase dimer that were quadrupole selected from a mixture of those two proteins. **(e)** Zoom in of **(b)** that shows the precursors and products from the first three CAPTR events. Note that there is a contaminate originating from the enolase sample (sharp peaks, not labeled)

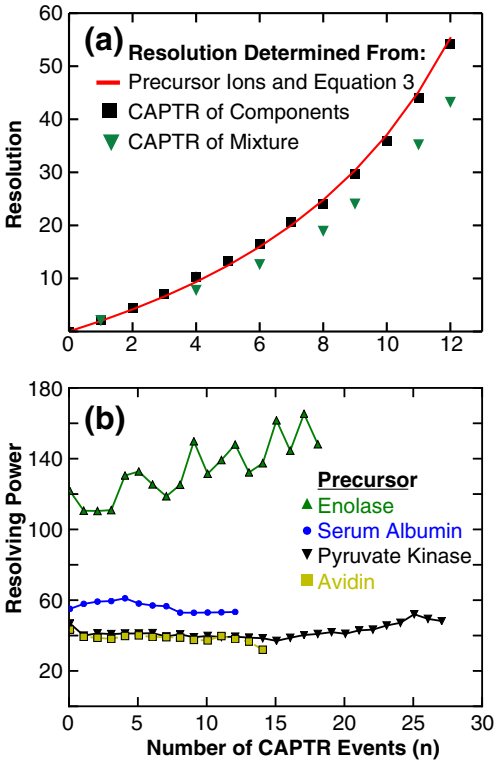

Figure 5. **(a)** Resolution of (serum albumin + (15 – n)H)$^{(15-n)+}$ and (enolase dimer + (21 – n)H)$^{(21-n)+}$ as a function of the number of CAPTR events (n) determined from the individual components (from Figure 4b–c, *black squares*), from the components in a mixture (from Figure 4d, *green triangles*), and from Equation (3) using parameters for the individual precursor ions (*red line*). Note that values for resolution of the components in a mixture were only determined for peaks with no interferences. **(b)** Resolving powers of enolase (results from Figure 4c), serum albumin (Figure 4b), pyruvate kinase (Figure 3), and avidin (Figure 2e)

the individual components, which suggests poorer ion desolvation for the former experiments. Note that values for the mixture were only determined when the centroids and widths could be determined unambiguously (i.e., there were not any interferences from other CAPTR products).

Origin of Increasing Resolution with Each Consecutive CAPTR Event

The resolution of two peaks depends on the widths and centroids of their respective m/z distributions (Equation (1)), and therefore the relationship between resolution and the number of CAPTR events can be determined from the effect that each CAPTR event has on the width and centroid of the resulting product m/z distributions. The relative increase in peak width between two different charge states may be described as a ratio,

$$\frac{\sigma_{z^*-n}}{\sigma_{z^*}} = \frac{z^*}{z^*-n} \tag{2}$$

where n is the number of CAPTR events and z^* is the charge state of the initial precursor ion. This relationship is based on time-of-flight fundamentals [58] and is established in greater detail in the Electronic Supplementary Material. Substituting Equation (2) into Equation (1) and assuming the centroids of the peaks shift solely because of the change in charge state yields

resolution as a function of the number of CAPTR events:

$$R_{CAPTR}(n) = \frac{\frac{m_x}{\left(z_x^*-n\right)} - \frac{m_y}{\left(z_y^*-n\right)}}{2\left[\sigma_x^*\left(\frac{z_x^*}{z_x^*-n}\right) + \sigma_y^*\left(\frac{z_y^*}{z_y^*-n}\right)\right]} \quad (3)$$

Using values of σ_x and σ_y determined from the individual precursor spectra (Figure 4b and c), Equation (3) was plotted in Figure 5a. This function yields values that are very similar to those determined from the individual CAPTR spectra (Figure 4b and c), indicating that this function can be used to accurately predict the performance of CAPTR-based separations. Furthermore, this agreement suggests that the changes in peak widths are primarily attributable to time-of-flight effects (i.e., contributions from anion adduction or desolvation are not significant).

One consequence of Equation (3) is that for precursor ions that have identical charge states (i.e., $z_x^*=z_y^*$), the resolution of the CAPTR products will not depend on the number of CAPTR events. Electronic Supplementary Material Figure S5 shows that all the CAPTR products from serum albumin and enolase dimer that have identical charge states have a resolution of ~30. In this case, resolution remains constant because the widths of the peaks change in unison with the *m*/*z* values, as predicted by Equation (2). Figure 5b shows the resolving power of enolase dimer (determined from the results shown in Figure 4b), serum albumin (Figure 4c), avidin (Figure 1e), and pyruvate kinase (Figure 3) as a function of the number of CAPTR events (n), where resolving power (R_p) is defined as:

$$Resolving\ \ Power = R_p = \frac{m/z}{4\sigma} \quad (4)$$

Note that R_p is expressed in terms of the width at the base of the peak (4σ), rather than the full width of the peak at half of its maximum height (2.355σ), to enable facile comparison with the values determined using Equations (1) and (3). The resolving powers measured for avidin (~40), pyruvate kinase (~40), and serum albumin (~55) do not depend strongly on the number of CAPTR events, whereas the values measured for enolase dimer increase from ~120 to ~150 with increasing numbers of CAPTR events.

These results show that after each CAPTR event, the relative increase in *m*/*z* is similar to the relative increase in the width of the peak. In contrast, in most reflectron time-of-flight mass spectrometry experiments, the resolving power of ions increase with increasing charge state, which is attributed to their increased kinetic energy and reflectron penetration [59]. One explanation is that the resolving powers for CAPTR products are limited by similar initial distributions of kinetic energy [58] (e.g., all CAPTR product ions experience similar aerodynamic acceleration during their introduction into the time-of-flight mass analyzer). Another explanation for these results is that the experimental distribution of *m*/*z* may be limited by the true distribution of *m*, which is consistent with incomplete desolvation during ionization and/or the adduction of molecules and ions from solution [60].

Conclusions

These results demonstrate that CAPTR is an extremely powerful complement to the mass spectrometry toolbox for analyzing proteins and protein complexes, particularly those in mixtures. This work benefits greatly from the pioneering efforts of McLuckey and coworkers in elucidating many aspects of the thermodynamics, kinetics, and analytical utility of proton transfer reactions for smaller analytes using ion traps [36, 43]. In this study, we demonstrated that the controlled charge reduction of *m*/*z*-selected native-like ions by CAPTR can increase the accuracy of charge state assignments and the resolution of interfering species in native mass spectrometry. The CAPTR product ion spectra for pyruvate kinase exhibit ~30 peaks and enable unambiguous determination of the charge state of each peak, whereas the corresponding precursor spectra exhibit ~6 peaks and the assigned charge states have an uncertainty of ±3%. 15+ serum albumin and 21+ enolase dimer both appear near *m*/*z* 4450 and have a resolution of 0.016. After isolation, each consecutive CAPTR event results in product ions whose resolution increases monotonically. After 12 CAPTR events, 3+ serum albumin and 9+ yeast enolase dimer have a resolution of 54, which is 3000-fold greater than that for the precursors. Additional tools for separating the components of congested mass spectra will be of great utility for a wide range of applications (e.g, the analysis of ribosomal complexes, viral capsids, polydisperse proteins, and protein complexes expressed under endogenous conditions).

CAPTR offers many benefits for reducing the charge states of native-like ions of proteins and protein complexes. First, the reactions are performed inside the mass spectrometer, which decouples the charge reduction and ionization processes and enables additional gas-phase manipulations (e.g., *m*/*z* selection of the cation and anion reactants, ion activation, and ion chemistry) prior to charge reduction. In contrast, performing charge reduction at atmospheric pressure results in the charge reduction of all components of the sample (potentially creating new interferences) and the increased formation of nonspecific aggregation because of a smaller fraction of droplets reaching the Rayleigh limit [61]. Second, the abundance of the $[PDCH–F]^-$ anions can be rapidly modulated or even completely cleared in seconds. These factors are very different than those for ion/neutral reactions, which typically exhibit substantial hysteresis when the pressure or identity of the neutral is varied. Third, $[PDCH–F]^-$ anions strongly favor proton transfer over electron transfer. Electron capture [54, 55, 62] by or electron transfer

[56] to the analyte can also yield product ions with lower charge states, but can also result in the cleavage of covalent bonds. The latter can provide additional molecular insights [54–56], but at the expense of increasing the complexity of the product ion spectra in ways that make it more challenging to assign charge states and probe the composition of mixtures. The combined attributes of CAPTR (i.e., performing reactions inside a hybrid mass spectrometer using a proton acceptor with specific chemistry whose abundance can be modulated rapidly), results in a high performance analytical platform for characterizing samples containing high mass and heterogeneous analytes.

Acknowledgments

Research reported in this publication was supported by the American Society for Mass Spectrometry (Research Award to M.F.B.), the National Institute of General Medical Sciences of the National Institutes of Health under Award Number T32GM008268, and the ARCS Foundation.

References

1. Loo, J.A.: Studying noncovalent protein complexes by electrospray ionization mass spectrometry. Mass Spectrom. Rev. **16**, 1–23 (1997)
2. Hofstadler, S.A., Sannes-Lowery, K.A.: Applications of ESI-MS in drug discovery: interrogation of noncovalent complexes. Nat. Rev. Drug Discov. **5**, 585–595 (2006)
3. Heck, A.J.R.: Native mass spectrometry: a bridge between interactomics and structural biology. Nat. Methods **5**, 927–933 (2008)
4. Hilton, G.R., Benesch, J.L.P.: Two decades of studying non-covalent biomolecular assemblies by means of electrospray ionization mass spectrometry. J. R. Soc. Interface **9**, 801–816 (2012)
5. Smith, D.P., Radford, S.E., Ashcroft, A.E.: Elongated oligomers in β2-microglobulin amyloid assembly revealed by ion mobility spectrometry-mass spectrometry. Proc. Natl. Acad. Sci. U. S. A. **107**, 6794–6798 (2010)
6. Bleiholder, C., Dupuis, N.F., Wyttenbach, T., Bowers, M.T.: Ion mobility-mass spectrometry reveals a conformational conversion from random assembly to β-sheet in amyloid fibril formation. Nat. Chem. **3**, 172–177 (2011)
7. Walldén, K., Williams, R., Yan, J., Lian, P.W., Wang, L., Thalassinos, K., Orlova, E.V., Waksman, G.: Structure of the VirB4 ATPase, alone and bound to the core complex of a type IV secretion system. Proc. Natl. Acad. Sci. U. S. A. **109**, 11348–11353 (2012)
8. Lu, C., Turley, S., Marionni, S.T., Park, Y.-J., Lee, K.K., Patrick, M., Shah, M., Sandkvist, M., Bush, M.F., Hol, W.G.J.: Hexamers of the Type II secretion ATPase GspE from *Vibrio cholerae* with increased ATPase activity. Structure **21**, 1707–1717 (2013)
9. Ekeowa, U.I., Freeke, J., Miranda, E., Gooptu, B., Bush, M.F., Perez, J., Teckman, J., Robinson, C.V., Lomas, D.A.: Defining the mechanism of polymerization in the serpinopathies. Proc. Natl. Acad. Sci. U. S. A. **107**, 17146–17151 (2010)
10. Aquilina, J.A., Benesch, J.L.P., Bateman, O.A., Slingsby, C., Robinson, C.V.: Polydispersity of a mammalian chaperone: mass spectrometry reveals the population of oligomers in αB-crystallin. Proc. Natl. Acad. Sci. U. S. A. **100**, 10611–10616 (2003)
11. Stengel, F., Baldwin, A.J., Bush, M.F., Hilton, G.R., Lioe, H., Basha, E., Jaya, N., Vierling, E., Benesch, J.L.P.: Dissecting heterogeneous molecular chaperone complexes using a mass spectrum deconvolution approach. Chem. Biol. **19**, 599–607 (2012)
12. Tito, M.A., Tars, K., Valegard, K., Hajdu, J., Robinson, C.V.: Electrospray time-of-flight mass spectrometry of the intact MS2 virus capsid. J. Am. Chem. Soc. **122**, 3550–3551 (2000)
13. Uetrecht, C., Barbu, I.M., Shoemaker, G.K., van Duijn, E., Heck, A.J.R.: Interrogating viral capsid assembly with ion mobility-mass spectrometry. Nat. Chem. **3**, 126–132 (2011)
14. Pierson, E.E., Keifer, D.Z., Selzer, L., Lee, L.S., Contino, N.C., Wang, J.C.-Y., Zlotnick, A., Jarrold, M.F.: Detection of late intermediates in virus capsid assembly by charge detection mass spectrometry. J. Am. Chem. Soc. **136**, 3536–3541 (2014)
15. Mann, M., Meng, C.K., Fenn, J.B.: Interpreting mass spectra of multiply charged ions. Anal. Chem. **61**, 1702–1708 (1989)
16. Reinhold, B.B., Reinhold, V.N.: Electrospray ionization mass spectrometry: deconvolution by an entropy-based algorithm. J. Am. Soc. Mass Spectrom. **3**, 207–215 (1992)
17. Ferrige, A.G., Seddon, M.J., Green, B.N., Jarvis, S.A., Skilling, J., Staunton, J.: Disentangling electrospray spectra with maximum entropy. Rapid Commun. Mass Spectrom. **6**, 707–711 (1992)
18. Stephenson, J.L., McLuckey, S.A.: Charge manipulation for improved mass determination of high-mass species and mixture components by electrospray mass spectrometry. J. Mass Spectrom. **33**, 664–672 (1998)
19. Morgner, N., Robinson, C.V.: Massign: An assignment strategy for maximizing information from the mass spectra of heterogeneous protein assemblies. Anal. Chem. **84**, 2939–2948 (2012)
20. Marty, M.T., Baldwin, A.J., Marklund, E.G., Hochberg, G.K.A., Benesch, J.L.P., Robinson, C.V.: Bayesian deconvolution of mass and ion mobility spectra: from binary interactions to polydisperse ensembles. Anal. Chem. **87**, 4370–4376 (2015)
21. Zhou, M., Wysocki, V.H.: Surface induced dissociation: dissecting noncovalent protein complexes in the gas phase. Acc. Chem. Res. **47**, 1010–1018 (2014)
22. Pagel, K., Hyung, S.-J., Ruotolo, B.T., Robinson, C.V.: Alternate dissociation pathways identified in charge-reduced protein complex ions. Anal. Chem. **82**, 5363–5372 (2010)
23. Felitsyn, N., Kitova, E.N., Klassen, J.S.: Thermal decomposition of a gaseous multiprotein complex studied by blackbody infrared radiative dissociation. Investigating the origin of the asymmetric dissociation behavior. Anal. Chem. **73**, 4647–4661 (2001)
24. Uetrecht, C., Versluis, C., Watts, N.R., Roos, W.H., Wuite, G.J.L., Wingfield, P.T., Steven, A.C., Heck, A.J.R.: High-resolution mass spectrometry of viral assemblies: molecular composition and stability of dimorphic hepatitis B virus capsids. Proc. Natl. Acad. Sci. U. S. A. **105**, 9216–9220 (2008)
25. Ma, X., Lai, L.B., Lai, S.M., Tanimoto, A., Foster, M.P., Wysocki, V.H., Gopalan, V.: Uncovering the stoichiometry of Pyrococcus furiosus RNase P, a multi-subunit catalytic ribonucleoprotein complex, by surface-induced dissociation and ion mobility mass spectrometry. Angew. Chem. Int. Ed. **53**, 11483–11487 (2014)
26. Ma, X., Zhou, M., Wysocki, V.H.: Surface induced dissociation yields quaternary substructure of refractory noncovalent phosphorylase B and glutamate dehydrogenase complexes. J. Am. Soc. Mass Spectrom. **25**, 368–379 (2014)
27. Lemaire, D., Marie, G., Serani, L., Laprévote, O.: Stabilization of gas-phase noncovalent macromolecular complexes in electrospray mass spectrometry using aqueous triethylammonium bicarbonate buffer. Anal. Chem. **73**, 1699–1706 (2001)
28. Lomeli, S.H., Yin, S., Ogorzalek Loo, R.R., Loo, J.A.: Increasing charge while preserving noncovalent protein complexes for ESI-MS. J. Am. Soc. Mass Spectrom. **20**, 593–596 (2009)
29. Sterling, H.J., Daly, M.P., Feld, G.K., Thoren, K.L., Kintzer, A.F., Krantz, B.A., Williams, E.R.: Effects of supercharging reagents on noncovalent complex structure in electrospray ionization from aqueous solutions. J. Am. Soc. Mass Spectrom. **21**, 1762–1774 (2010)
30. Bornschein, R., Hyung, S.-J., Ruotolo, B.: Ion mobility-mass spectrometry reveals conformational changes in charge reduced multiprotein complexes. J. Am. Soc. Mass Spectrom. **22**, 1690–1698 (2011)
31. Allen, S.J., Schwartz, A.M., Bush, M.F.: Effects of polarity on the structures and charge states of native-like proteins and protein complexes in the gas phase. Anal. Chem. **85**, 12055–12061 (2013)
32. McLuckey, S.A., Goeringer, D.E.: Ion/molecule reactions for improved effective mass resolution in electrospray mass spectrometry. Anal. Chem. **67**, 2493–2497 (1995)
33. Schnier, P.D., Gross, D.S., Williams, E.R.: Electrostatic forces and dielectric polarizability of multiply protonated gas-phase cytochrome *c* ions probed by ion/molecule chemistry. J. Am. Chem. Soc. **117**, 6747–6757 (1995)
34. Ogorzalek Loo, R.R., Udseth, H.R., Smith, R.D.: A new approach for the study of gas-phase ion-ion reactions using electrospray ionization. J. Am. Soc. Mass Spectrom. **3**, 695–705 (1992)

35. Stephenson, J.L., McLuckey, S.A.: Ion/ion reactions in the gas phase: proton transfer reactions involving multiply-charged proteins. J. Am. Chem. Soc. **118**, 7390–7397 (1996)
36. McLuckey, S.A., Stephenson, J.L.: Ion/ion chemistry of high-mass multiply charged ions. Mass Spectrom. Rev. **17**, 369–407 (1998)
37. Scalf, M., Westphall, M.S., Krause, J., Kaufman, S.L., Smith, L.M.: Controlling charge states of large ions. Science **283**, 194–197 (1999)
38. Ebeling, D.D., Westphall, M.S., Scalf, M., Smith, L.M.: Corona discharge in charge reduction electrospray mass spectrometry. Anal. Chem. **72**, 5158–5161 (2000)
39. Campuzano, I.G., Schnier, P.: Coupling electrospray corona discharge, charge reduction and ion mobility mass spectrometry: from peptides to large macromolecular protein complexes. Int. J. Ion Mobil. Spectrom. **16**, 51–60 (2013)
40. McLuckey, S.A., Glish, G.L., Van Berkel, G.J.: Charge determination of product ions formed from collision-induced dissociation of multiply protonated molecules via ion/molecule reactions. Anal. Chem. **63**, 1971–1978 (1991)
41. Herron, W.J., Goeringer, D.E., McLuckey, S.A.: Product ion charge state determination via ion/ion proton transfer reactions. Anal. Chem. **68**, 257–262 (1996)
42. Herron, W.J., Goeringer, D.E., McLuckey, S.A.: Ion-ion reactions in the gas phase: proton transfer reactions of protonated pyridine with multiply charged oligonucleotide anions. J. Am. Chem. Soc. **6**, 529–532 (1995)
43. Pitteri, S.J., McLuckey, S.A.: Recent developments in the ion/ion chemistry of high-mass multiply charged ions. Mass Spectrom. Rev. **24**, 931–958 (2005)
44. Williams, J.P., Brown, J.M., Campuzano, I., Sadler, P.J.: Identifying drug metallation sites on peptides using electron transfer dissociation (ETD), collision induced dissociation (CID) and ion mobility-mass spectrometry (IM-MS). Chem. Commun. **46**, 5458–5460 (2010)
45. Zhao, Q., Soyk, M.W., Schieffer, G.M., Fuhrer, K., Gonin, M.M., Houk, R.S., Badman, E.R.: An ion trap-ion mobility-time of flight mass spectrometer with three ion sources for ion/ion reactions. J. Am. Soc. Mass Spectrom. **20**, 1549–1561 (2009)
46. Sobott, F., McCammon, M.G., Robinson, C.V.: Gas-phase dissociation pathways of a tetrameric protein complex. Int. J. Mass Spectrom. **230**, 193–200 (2003)
47. McLuckey, S.A., Stephenson, J.L., Asano, K.G.: Ion/ion proton-transfer kinetics: implications for analysis of ions derived from electrospray of protein mixtures. Anal. Chem. **70**, 1198–1202 (1998)
48. Wu, J., Hager, J.W., Xia, Y., Londry, F.A., McLuckey, S.A.: Positive ion transmission mode ion/ion reactions in a hybrid linear ion trap. Anal. Chem. **76**, 5006–5015 (2004)
49. Stephenson, J.L., Van Berkel, G.J., McLuckey, S.A.: Ion-ion proton transfer reactions of bio-ions involving noncovalent interactions: holomyoglobin. J. Am. Soc. Mass Spectrom. **8**, 637–644 (1997)
50. Sterner, J.L., Johnston, M.V., Nicol, G.R., Ridge, D.P.: Apparent proton affinities of highly charged peptide ions. J. Am. Soc. Mass Spectrom. **10**, 483–491 (1999)
51. Bouchoux, G.: Gas phase basicities of polyfunctional molecules. Part 3: amino acids. Mass Spectrom. Rev. **31**, 391–435 (2012)
52. Gunawardena, H.P., He, M., Chrisman, P.A., Pitteri, S.J., Hogan, J.M., Hodges, B.D.M., McLuckey, S.A.: Electron transfer versus proton transfer in gas-phase ion/ion reactions of polyprotonated peptides. J. Am. Chem. Soc. **127**, 12627–12639 (2005)
53. Chrisman, P.A., Pitteri, S.J., Hogan, J.M., McLuckey, S.A.: $SO_2^{\cdot-}$ electron transfer ion/ion reactions with disulfide linked polypeptide ions. J. Am. Soc. Mass Spectrom. **16**, 1020–1030 (2005)
54. Zhang, H., Cui, W., Wen, J., Blankenship, R.E., Gross, M.L.: Native electrospray and electron-capture dissociation FTICR mass spectrometry for top-down studies of protein assemblies. Anal. Chem. **83**, 5598–5606 (2011)
55. Li, H., Wolff, J.J., Van Orden, S.L., Loo, J.A.: Native top-down electrospray ionization-mass spectrometry of 158 kDa protein complex by high-resolution Fourier transform ion cyclotron resonance mass spectrometry. Anal. Chem. **86**, 317–320 (2014)
56. Lermyte, F., Williams, J.P., Brown, J.M., Martin, E.M., Sobott, F.: Extensive charge reduction and dissociation of intact protein complexes following electron transfer on a quadrupole-ion mobility-time-of-flight MS. J. Am. Soc. Mass Spectrom. **26**, 1069–1076 (2015)
57. Stephenson, J.L., McLuckey, S.A.: Ion/ion proton transfer reactions for protein mixture analysis. Anal. Chem. **68**, 4026–4032 (1996)
58. Guilhaus, M.: Principles and instrumentation in time-of-flight mass spectrometry. J. Mass Spectrom. **30**, 1519–1532 (1995)
59. Cornish, T.J., Cotter, R.J.: High-order kinetic energy focusing in an end cap reflectron time-of-flight mass spectrometer. Anal. Chem. **69**, 4615–4618 (1997)
60. McKay, A.R., Ruotolo, B.T., Ilag, L.L., Robinson, C.V.: Mass measurements of increased accuracy resolve heterogeneous populations of intact ribosomes. J. Am. Chem. Soc. **128**, 11433–11442 (2006)
61. de la Mora, J.F., Ude, S., Thomson, B.A.: The potential of differential mobility analysis coupled to MS for the study of very large singly and multiply charged proteins and protein complexes in the gas phase. Biotechnol. J. **1**, 988–997 (2006)
62. Abzalimov, R.R., Kaltashov, I.A.: Electrospray ionization mass spectrometry of highly heterogeneous protein systems: protein ion charge state assignment via incomplete charge reduction. Anal. Chem. **82**, 7523–7526 (2010)